

Solving a Set of Truncated Dyson-Schwinger Equations with a Globally Converging Method

Axel Maas

Gesellschaft für Schwerionenforschung mbH, Planckstr. 1, D-64291 Darmstadt, Germany

Abstract

A globally converging numerical method to solve coupled sets of non-linear integral equations is presented. Such systems occur e.g. in the study of Dyson-Schwinger equations of Yang-Mills theory and QCD. The method is based on the knowledge of the qualitative properties of the solution functions in the far infrared and ultra-violet. Using this input, the full solutions are constructed using a globally convergent modified Newton iteration. Two different systems will be treated as examples: The Dyson-Schwinger equations of 3-dimensional Yang-Mills-Higgs theory provide a system of finite integrals, while those of 4-dimensional Yang-Mills theory at high temperatures are only finite after renormalization.

Key words: Dyson Schwinger equations, Nonlinear integral equations, Globally convergent solution methods, Numerical solution methods, Coupled sets of integral equations

PACS: 02.30.Rz Integral equations, 02.60.Cb Numerical simulation; solution of equations, 11.15.Tk Other nonperturbative techniques

1 Introduction

Integral equations appear in many areas of physics, and they are ubiquitous in non-perturbative field theory. Most prominent examples are the Dyson-Schwinger equations (DSEs). These equations form coupled sets of non-linear integral equations, which must be solved self-consistently to make progress beyond resummed perturbation theory. Solutions to these equations thus lie at

Email address: `Axel.Maas@Physik.TU-Darmstadt.de` (Axel Maas).

the heart of many truly non-perturbative calculations. E.g. in the low-energy regime of QCD, the study of the DSEs has provided a wealth of physical insight, see e.g. ref. [1] for a review. To solve these equations, fast and reliable algorithms are desirable, which minimize the required prior knowledge.

While the theory of single linear integral equations with well-behaved integral kernels is well understood, see e.g. [2], this is not the case for typical equations in field theories. These are normally coupled sets of non-linear equations with integrable, but singular integral kernels and not necessarily well-behaved solutions.

In many problems where solutions are only searched on a compact manifold, discretization of the integral equations allow to solve them by fix-point iteration methods. This is especially the case in non-relativistic settings, such as condensed matter problems. In fully relativistic settings, such solutions are plagued by finite volume effects and discretization errors for extremely large and extremely small momenta. This is in some cases of no importance, but in the case of non-abelian gauge theories, these regions are of special interest, as they are the origins of non-perturbative phenomena and of matching to perturbation theory. Nonetheless, methods using discretization provide a wealth of valuable informations also in these cases, see e.g. refs. [3,4,5,6].

The aim here is to construct a globally convergent method applicable to such problems. In this paper section 2 will layout the DSEs to be solved and thus set the mathematical frame¹. The numerical method, including the implementation, will be discussed for two different systems. A finite system is obtained for 3-dimensional Yang-Mills-Higgs theory. It is treated in section 3. In section 3 also an explicit example will be shown. A renormalized system is obtained for finite-temperature 4-dimensional Yang-Mills theory to be discussed in section 4. In section 5 some concluding remarks are made. Some technical details are deferred to an appendix. A thorough discussion of the physics case can be found in refs. [7,8,9].

2 Dyson-Schwinger equations

The complete content of a theory is given by the corresponding Green's functions. The Dyson-Schwinger equations [10] determine the Green's functions of a theory through an infinite set of coupled, non-linear integral equations.

¹ This section includes a short description of the derivation of the equations to be solved. If the reader is exclusively interested in the numerical method, this section can be mostly skipped, except for the systems of equations to be solved. These are given in (9-11) for the finite system and (15-17) for the renormalized system.

A theory is fully described by the Lagrangian density $\mathcal{L}(\phi^a, \partial_\mu \phi^a, \dots)$ of the fields ϕ^a and their derivatives, where a is a generic multi-index. The Green's functions² are then given by functional derivatives w.r.t. the fields ϕ^b of the identity

$$\int \mathcal{D}\phi \frac{\delta}{\delta \phi^a} \exp(-\int d^d x \mathcal{L}) = 0. \quad (1)$$

Here d is the number of space-time dimensions. See refs. [1,11] for a detailed introduction to DSEs.

It is in general not possible to solve all DSEs simultaneously, and it is therefore necessary to truncate the system to a finite number of equations. This entails nearly always violations of internal symmetries such as gauge symmetries, and it is an essentially non-trivial task to compensate or estimate these effects. For a detailed study of this problem, see e.g. refs. [1,6,7]. The consequences of these truncation and how to control them is a physical issue, which will not be treated here. The implementation of appropriate measures to deal with this problem can have impact on the numerical method. Furthermore, in quantum field theory, terms in the DSEs usually diverge, and must be made finite by renormalization [12]. Although this is again a physical issue, it has also consequences for the numerical method. Therefore some numerical aspects of both problems will be discussed briefly in section 4.

The presented numerical method has been applied successfully to two systems. One is 3-dimensional Yang-Mills theory coupled to an adjoint Higgs as the infinite-temperature limit of 4-dimensional Yang-Mills theory [7,8]. The second is 4-dimensional Yang-Mills theory at high temperature [7,9]. The first system is finite and the numerical problem thus will be treated first in section 3. The second requires renormalization and the necessary alterations will be discussed in section 4. In the following subsections, the Dyson-Schwinger equations of each system will be shortly introduced.

2.1 3-dimensional Yang-Mills theory coupled to an adjoint, massive Higgs

The infinite-temperature limit of 4-dimensional Yang-Mills theory is described by a 3-dimensional Yang-Mills theory coupled to an adjoint, massive Higgs field [13]. For physical reasons the choice of Landau gauge is advantageous, which will be made here exclusively. The Lagrangian of this system in Euclidean space is then given by [8,13]

$$\mathcal{L} = \frac{1}{4} F_{\mu\nu}^a F_{\mu\nu}^a + \bar{c}^a \partial_\mu D_\mu^{ab} c^b + \frac{1}{2} (D_\mu^{ab} \phi^b D_\mu^{ac} \phi^c + m_h^2 \phi^a \phi^a) + \frac{h}{4} \phi^a \phi^a \phi^b \phi^b, \quad (2)$$

² The discussion here is restricted to an Euclidean space-time, but can directly be transferred to any other metric.

with the field strength tensor $F_{\mu\nu}^a$ and the covariant derivative D_μ^{ab} defined as

$$F_{\mu\nu}^a = \partial_\mu A_\nu^a - \partial_\nu A_\mu^a - g_3 f^{abc} A_\mu^b A_\nu^c \quad (3)$$

$$D_\mu^{ab} = \delta^{ab} \partial_\mu + g_3 f^{abc} A_\mu^c. \quad (4)$$

A_μ^a is the 3-dimensional gluon field, c^a and \bar{c}^a are the Faddeev-Popov ghost and anti-ghost fields, ϕ^a is the Higgs field, g_3 is the dimensionful coupling, which is 1 in appropriate units, and $m_h \sim g_3^2$ is fixed by Monte Carlo calculations on discrete space-time lattices to be $0.88g_3^2$ [14]. The constants f^{abc} are the structure constants of the gauge group. In general, contributions stemming from the Higgs field could be divergent. However, this is not permissible when viewing the Lagrangian (2) as the infinite-temperature limit of 4-dimensional Yang-Mills theory. Therefore leading order perturbation theory requires that h is fixed to

$$h = -2g_3^2 \frac{C_A}{C_A + 2}, \quad (5)$$

where $C_A = f_{abc}f^{abc}$ is the adjoint Casimir of the gauge group.

The simplest non-vanishing Green's functions in this theory are obtained by deriving the identity (1) once more with respect to the fields. The inverse of these Green's functions are called propagators, and there is one for each field. These propagators D_G , $D_{\mu\nu}$, and D_H of the ghost, the gluon, and the Higgs, respectively, can be parameterized by three scalar functions, so-called dressing functions, G , Z , and H as

$$D_G(p^2) = \frac{-G(p^2)}{p^2} \quad (6)$$

$$D_{\mu\nu}(p) = \left(\delta_{\mu\nu} - \frac{p_\mu p_\nu}{p^2} \right) \frac{Z(p^2)}{p^2} \quad (7)$$

$$D_H(p^2) = \frac{H(p^2)}{p^2}, \quad (8)$$

respectively. The dressing functions G , Z , and H have to be positive semi-definite by the Gribov condition [8,15]. Using these dimensionless quantities instead of the propagators improves the numerical stability for large p significantly, as otherwise trivial kinematic effects would require an enormous precision.

The truncated DSEs are then obtained by standard techniques [1] in a straightforward but tedious way [7]. The tensor equation for the gluon propagator is contracted with an appropriate projector to yield a scalar equation. The projector is parameterized by a variable ζ , on which therefore the integral kernels depend. This yields the DSEs for the ghost dressing function G , the gluon dressing function Z , and the Higgs dressing function H

$$0 = 1 + \frac{g_3^2 C_A}{(2\pi)^2} \int d\theta dq A_T(p, q) G(q) Z(p - q) - \frac{1}{G(p)} \quad (9)$$

$$0 = 1 + \frac{m_h^2}{p^2} + T^{HG} + T^{HH} + \frac{g_3^2 C_A}{(2\pi)^2} \int d\theta dq \left(N_1(p, q) H(q) Z(p + q) + N_2(p, q) H(p + q) Z(q) \right) - \frac{1}{H(p)} \quad (10)$$

$$0 = 1 + T^{GH} + T^{GG} + \frac{g_3^2 C_A}{(2\pi)^2} \int d\theta dq \left(R(p, q) G(q) G(p + q) + M_L(p, q) H(q) H(p + q) + M_T(p, q) Z(q) Z(p + q) \right) - \frac{1}{Z(p)}, \quad (11)$$

where θ is the angle between p and q . The tadpoles T^{ij} are not independent functions but compensate any divergencies and thus render the equations (9-11) finite [7]. The integral kernels³ A_T , N_1 , N_2 , R , M_T , and M_L as well as the tadpoles are listed in appendix A. Trivial factors, such as the integral measure, have been included into the kernels. The kernels all have a very similar structure, being rational functions of the momenta. All these kernels furthermore contain integrable singularities of the type $1/(p - q)^m$ with some positive m .

2.2 Finite temperature Yang-Mills theory

The second example is finite temperature 4-dimensional Yang-Mills theory. In the Matsubara formalism [16] it is described by the (Euclidean) Lagrangian

$$\mathcal{L} = \frac{1}{4} F_{\mu\nu}^a F_{\mu\nu}^a + \bar{c}^a \partial_\mu D_\mu^{ab} c^b, \quad (12)$$

which is very similar to (2). The only difference to the previous example is replacing g_3 by the 4-dimensional dimensionless coupling g_4 in the field strength tensor (3) and the covariant derivative (4) and dropping the Higgs field. Using the Matsubara formalism [16] the DSEs of the vacuum [1] can be extended to finite temperature [7]. The propagators are again the most simple Green's functions and can be parameterized by also three functions

$$D_G(p) = \frac{-G(p_0^2, \vec{p}^2)}{p^2} \quad (13)$$

³ The kernel M_T in addition depends on a parameter δ_{3g} . It is fixed throughout to $1/4$ and parameterizes the constructed three-gluon vertex. Furthermore this induces an additional non-trivial dependence of M_T on G and Z , see appendix A and ref. [8].

for the ghost propagator and similarly for the gluon propagator as [16]

$$D_{\mu\nu}(p) = P_{T\mu\nu}(p) \frac{Z(p_0^2, \vec{p}^2)}{p^2} + P_{L\mu\nu}(p) \frac{H(p_0^2, \vec{p}^2)}{p^2}. \quad (14)$$

where P_T and P_L are projectors transverse and longitudinal w.r.t. the heat-bath [16]. The coincidence of the names of the dressing functions to those of the previous example is intentional. There is an exact correspondence in the limit of infinite temperature.

The truncated DSEs for the dressing functions G , Z , and H are obtained in the same way as before and read

$$0 = \tilde{Z}_3 + \frac{g_4^2 T C_A}{(2\pi)^2} \sum_{n=-\infty}^{\infty} \int d\theta dq \left(A_T^f(p, q) G(q) Z(p - q) + A_L^f(p, q) G(q) H(p - q) \right) - \frac{1}{G(p)} \quad (15)$$

$$0 = \xi Z_{3L} + T^{fHG} + T^{fHH} + \frac{g_4^2 T C_A}{(2\pi)^2} \sum_{n=-\infty}^{\infty} \int d\theta dq \left(P^f(p, q) G(q) G(p + q) + N_L^f(p, q) Z(q) Z(p + q) + N_1^f(p, q) H(q) Z(p + q) + N_2^f(p, q) H(p + q) Z(q) + N_T^f(p, q) H(q) H(p + q) \right) - \frac{\xi}{H(p)} \quad (16)$$

$$0 = Z_{3T} + T^{fGH} + T^{fGG} + \frac{g_4^2 T C_A}{(2\pi)^2} \sum_{n=-\infty}^{\infty} \int d\theta dq \left(R^f(p, q) G(q) G(p + q) + M_L^f(p, q) H(q) H(p + q) + M_1^f(p, q) H(q) Z(p + q) + M_2^f(p, q) H(p + q) Z(q) + M_T^f(p, q) Z(q) Z(p + q) \right) + \frac{p_0^2(\zeta - 1)}{2p^2} \left(Z_{3L} - \frac{1}{H(p)} \right) - \frac{1}{Z(p)}. \quad (17)$$

The temperature is denoted by T . The summation is performed over all integers n . In the Matsubara formalism the component q_0 is discrete and given by $q_0 = 2\pi T n$, called the Matsubara frequency. Also the external p_0 is thus discrete.

In the present case, the sum is truncated, and only the range $[-N + 1, N - 1]$ is included. Close inspection of the equations reveals further that the dressing functions can only depend on $|p_0|$ and $|\vec{p}|$. The corresponding symmetry, under $p_0 \rightarrow -p_0$, is used to reduce the number of equations significantly. Therefore $3N$ independent functions have to be determined. The largest system treated numerically so far is $N = 21$.

The kernels A_T^f , A_L^f , R^f , M_T^f , M_1^f , M_2^f , M_L^f , P^f , N_T^f , N_1^f , N_2^f , and N_L^f are rather lengthy, and will not be displayed here. They can be found in ref. [7].

The kernels are very similar in structure to their 3-dimensional pendants listed in appendix A. The same applies to the tadpoles T^{fij} , with the notable exception of the T^{fHj} . These are much more similar to the transverse expressions T^{fGj} than in the case of 3 dimensions. Especially these are now also determined by integrals, see ref. [7] again for details. The finite-temperature theory is renormalizable. Thus explicit wave-function renormalization constants \tilde{Z}_3 , Z_{3L} , and Z_{3T} have been introduced⁴.

The variables ζ and ξ are introduced by contraction of the equation of the gluon propagator with two different projectors [7,9] as before. These variables have been introduced to study the consequences of the truncation. For $p_0 = 0$, equation (16) is only superficially dependent on ξ : since all integral kernels are proportional to ξ , the dependence can be divided out for $\xi \neq 0$.

The renormalization constants are defined at a subtraction point s , which can be chosen arbitrarily, but for numerical reasons should be different from 0. The explicit implementation of the renormalization prescription [7,9] for the DSE of a dressing function $F = G, Z, H$ with self-energy contributions I

$$\frac{1}{F(p)} = 1 + I(p) \quad (18)$$

is then for the corresponding wave function renormalization constant Z_3

$$\frac{1}{F(p)} = 1 + \delta Z_3 + I(p) \quad (19)$$

$$\delta Z_3 = -I(s) \quad (20)$$

$$Z_3 = 1 + \delta Z_3 \quad (21)$$

and in the case of $H(0, |\vec{p}|)$

$$\frac{1}{H(0, |\vec{p}|)} = 1 + \delta Z_{3L} + \frac{\delta m^2}{p^2} + I(p) \quad (22)$$

$$\delta m^2 = m_r^2 - \lim_{p \rightarrow 2\delta} p^2 I(p) \quad (23)$$

$$\delta Z_{3L} = -I(s) + \frac{\lim_{p \rightarrow 2\delta} p^2 I(p)}{s^2}, \quad (24)$$

where $m_r = m_{3d}$ is the renormalized mass, and δ is an infinitesimal parameter, different from zero only for numerical reasons. It is taken to be the same value as the infrared integral cutoff introduced in the next section. The difference compared to performing the subtraction at 0 is negligible. Note that due to the truncation of the Matsubara sum the wave function renormalization constants

⁴ No vertex renormalization occurs within this truncated system.

depend on p_0 . This dependence vanishes for $N \rightarrow \infty$ [9], but has to be taken into account in the numerical treatment presented here.

3 Numerical method

The numerical technique to solve the system of equations (9-11) and (15-17) are very similar. Renormalization in the 4-dimensional system (15-17) requires some extensions. Therefore here only the finite system will be treated. The modifications for the renormalized system will be discussed in section 4.

The earliest approach to solve the 4-dimensional equivalent (without the additional Higgs field) of system (9-11) was based on a direct iteration method [17]. This has afterwards been replaced by a method based on a local Newton iteration [6,18,19]. The latter approach used as starting inputs for a local iteration results obtained from a discretized version of the problem [3]. The method presented here generalizes this ansatz to provide global convergence and remove the necessity of input data. For the sake of completeness the full method will be described here, although several elements have been taken from the previous one.

The basis for the numerical treatment is an analytical investigation of the asymptotic behavior of the solutions. This will be discussed in subsection 3.1. An important ingredient is the representation of the solutions using their asymptotics. This and the integration method will be discussed in subsection 3.2. The heart of the method is the iteration procedure, which will be described in subsection 3.3. Some notes on the efficient implementation are given in subsection 3.4. An explicit calculation with a typical set of numerical parameters is given as an example in section 3.5.

3.1 Analytical foundation

It is important to gather as many analytical properties as possible to obtain an appropriate representation of the solutions. Especially using as few parameters as possible permits to obtain maximal numerical efficiency.

The searched for positive semi-definite solution functions are continuously differentiable and analytical in the momentum range $(0, \infty)$. For physical reasons no poles at intermediate momenta are expected. However the solutions are not bounded from above. Thus divergences at $p = 0$ are possible. Therefore the infrared asymptotic behavior is of special interest. Favorable, it turns out that the leading asymptotic behavior can be obtained analytically [7,8,20].

In the infrared, power-like ansätze can be used [8,20]⁵,

$$\lim_{p \rightarrow 0} F(p) = A_F(p^2)^{-e_F}. \quad (25)$$

This is possible due to the singularity structure $1/(p-q)^m$ of the integral kernels, which lead to a domination of the integrals by momenta of order $q \approx p$. It is hence allowed to replace the dressing functions by the ansätze (25). It is then possible to solve the massless integrals analytically [8,20]. The Higgs propagator is dominated by the renormalized mass term in equation (10) and thus has the unique exponent $e_H = -1$. This also determines A_H uniquely [8]. There are two possible solutions for the ghost exponents. One of the solution is $e_G = 1/2$, while the other depends on ζ and varies as $e_G \in (1/4, 1/2]$. The gluon exponent e_Z is not independent, but related to e_G by [8,20]

$$e_G = -\frac{1}{2} \left(e_Z + \frac{1}{2} \right). \quad (26)$$

The coefficients A_G and A_Z cannot be determined uniquely. However, they are related by [8]

$$\begin{aligned} \frac{1}{A_G^2 A_Z} &= \frac{C_A g_3^2}{(4\pi)^{\frac{3}{2}}} \frac{2^{4(e_G-1)} (2 + 2e_G(\zeta - 1) - \zeta) \Gamma(2 - 2e_G) \sin^2(\pi e_G)}{\cos(2\pi e_G) (e_G - 1) e_G^2 \Gamma(\frac{3}{2} - 2e_G)} \\ &\equiv \frac{1}{J(e_G, \zeta)}. \end{aligned} \quad (27)$$

Furthermore, in the ultraviolet, $p \gg g_3^2$, an analytic solution can be obtained by perturbation theory due to asymptotic freedom [8]. The dressing functions are then given by

$$\lim_{p \rightarrow \infty} F(p) = 1 + \frac{w_F g_3^2 C_A}{p}, \quad (28)$$

The w_F are the positive constants $w_G = 1/16$, $w_Z = 9/64$ and $w_H = 1/4$. Note that in contrast to 4 dimensions these are already the resummed solutions, as leading order and leading order resummed perturbation theory in 3-dimensional Yang-Mills theory are the same [8]. This concludes the list of known analytical properties of the solutions.

3.2 Expansion and integration

The first step is to describe the solutions in terms of known functions. The solutions are due to their ultraviolet behavior neither integrable nor square-integrable. This prohibits an expansion in any orthogonal set of polynomials.

⁵ Note that this is very similar to the case of 4 dimensions [21].

This problem is reinforced by the infrared divergence of the ghost dressing function.

Therefore originally [18,22] the dressing functions were expanded as

$$F(p) = \theta(\varepsilon - p)D_F^I(p) + \theta(p - \varepsilon)\theta(\Lambda - p)D_F^N(p) + \theta(p - \Lambda)D_F^U(p) \quad (29)$$

$$\ln(D_i^N(p)) = \sum_{j=0}^{N_{ch}} c_{ij} T_j(M(p)) \quad (30)$$

where D_F^I denotes the analytical infrared solution (25) and D_F^U the analytical ultraviolet solution (28). The index i runs through 1, 2, 3 corresponding to G , Z , and H , respectively. The range $[\varepsilon, \Lambda]$ is covered by a numerical expansion⁶ in N_{ch} Chebychef polynomials T_j . Good results can be achieved with $N_{ch} = 30 - 40$. For special purposes like computation of Schwinger functions or thermodynamic quantities [8] $N_{ch} = 100 - 500$ are used.

The typical expansion range in the case of 3 dimensions is chosen to be $[\varepsilon, \Lambda] = [10^{-2}g_3^2, 2 \cdot 10^3 g_3^2]$. The function M in (30) is a suitable mapping function which maps the momenta to the domain $(-1, 1)$ of the Chebychef polynomials. Since the dressing functions $F = G, Z, H$ vary on logarithmic scales, the mapping function is chosen accordingly as⁷

$$M(p) = A + B \ln(p) \quad (31)$$

where A and B are chosen such as to yield

$$M^{-1}(\varepsilon) = z_0 \quad (32)$$

$$M^{-1}(\Lambda) = z_{N_{ch}}, \quad (33)$$

where M^{-1} is the inverse function of (31) and z_i are the i th zero of the Chebychef polynomial of order N_{ch} .

To increase the numerical stability, (29) is altered to

⁶ Expanding the logarithm instead of the function itself leads to a considerable smoothing at large momenta and the number of needed Chebychef polynomials drastically decreases.

⁷ An alternative is a conformal mapping like $z/(z+1)$ which removes the necessity of a numerical upper and lower cutoff of the integrals. However, such a mapping does not provide any advantage beyond formal elegance and in addition did not provide as well spaced evaluation points as the logarithmic mapping.

Dressing function (F)	a_F	b_F	c_F
Ghost (G)	1	ν^{2e_G}	ν
Gluon (Z)	ν	ν	$2/\nu^{2e_Z}$
Higgs (H)	1	m_r^2	0

Table 1

The coefficients for the fitting functions (35-37) in terms of the scale of the problem ν and of the renormalized Higgs mass m_r [8].

$$D_F(p) = \theta(\varepsilon - p)D_F^I(p) + \theta(p - \varepsilon)\theta(\Lambda - p)D_F^N(p)f_F(p) + \theta(p - \Lambda)D_F^U(p) \quad (34)$$

where the f_F interpolate between the qualitative behavior of D_F^I and D_F^U . Thus for divergent quantities like the ghost dressing function

$$f_G(p) = 1 + \frac{a_G}{p^{-2e_G}} \frac{b_G + p^{-2e_G}}{c_G + p} \quad (35)$$

with suitably chosen fitting constants a_G , b_G , c_G . This especially improved the quality at large p , as it is notoriously difficult to fit with a polynomial onto a constant. Similar for converging quantities as the gluon and the Higgs the fits

$$f_Z(p) = \frac{p^{-2e_Z}}{c_Z + p^{-2e_Z}} \left(1 + \frac{a_Z}{b_Z + p} \right) \quad (36)$$

$$f_H(p) = \frac{a_H p^{-2e_H}}{p^{-2e_H} + c_H p + b_H^2} \quad (37)$$

are used, respectively. Note that it turns out to be more stable to neglect in the case of the Higgs the subleading contributions in (28) fitted by c_H . The coefficients are chosen to resemble the typical scale ν for the system investigated. In case of the 3-dimensional theory this is $\nu = g_3^2$ while in case of the 4-dimensional system $\nu = g_4^2 T$. The coefficients can then be read off table 1 for the 3-dimensional theory. In the 4-dimensional theory a more simplified version of (35-37) is used, omitting the perturbative tail. For the hard modes, $p_0 \neq 0$, essentially a fit of type (37) is used.

Additionally it is necessary to choose an integrator. For the radial integral, after applying the logarithmic map (31) to the integration variable, Gauss-Legendre integration is sufficient [22]. Since the integrals are finite, a lower and upper numerical integral cutoff has been used, and the integration has been performed in $[\delta, \Omega]$, with $\delta \ll \varepsilon$ and $\Lambda \ll \Omega$, typically $[10^{-5}g_3^2, 10^7g_3^2]$. The remaining problem to be dealt with is the singularity structure of the integral kernels and of the ghost dressing function G . These appear at $|q| = 0$ and $p = \pm q$, depending on the equation. The $|q| = 0$ singularity is cured by imposing the lower cutoff. Here the logarithmic mapping of the integration

variable provides a sufficient sampling of the integrable singularities arising. More problematic is the singularity due to the coincidence with the external momentum. It can be removed by splitting the integral in two parts, up to and above p . Again the logarithmic spreading provides sufficient sampling of the integrable singularity. As p will only be chosen from $[\varepsilon, \Lambda]$ the integral is finally performed as

$$\int_0^\infty \rightarrow \int_\delta^\varepsilon + \int_\varepsilon^p + \int_p^\Lambda + \int_\Lambda^\Omega. \quad (38)$$

The angular integral is straightforward and can be done by normal Gauss-Legendre integration. However, it is necessary to perform the angular integral before the radial one, as some divergences cancel only due to the angular integration. These cancellations also require a sufficient sampling, leading to $N_a = 80$ points in angular direction and $N_\delta + N_\varepsilon + N_p + N_\Lambda = 60 + 100 + 100 + 60 = 320$ points in radial direction as typical values.

3.3 Micro-, Macro, and Super-cycles

Originally, solutions for the set of coefficients c_{ij} were obtained using a local Newton iteration procedure [18]. The presented method here uses instead a global Newton method with back-tracking [23]. This approach is very insensitive to the starting value, and a typical starting guess is $c_{ij} = 0$. The necessary $3N_{ch}$ functions to determine the coefficients c_{ij} are obtained by evaluating the system of equations (9-11) at the zeros of $T_{N_{ch}}$. At these points the expansion in Chebychevs is exact. This also entails that all evaluation points stem from $[\varepsilon, \Lambda]$. This makes it even more necessary to know the behavior of the functions outside this domain analytically to perform the integrals in the intervals $[\delta, \varepsilon]$ and $[\Lambda, \Omega]$.

Therefore the numerical problem was to solve the $3N_{ch}$ non-linear equations for the coefficients c_{ij} and determine the coefficient A_G . These equations can be collected generically into an equation vector \vec{E} , with components defined as

$$E_{(i-1)N_{ch}+j} = \tau(p_j) + \sum_{l=1}^3 I(F_i, F_l, p_j) - \frac{1}{F_i(p_j)} \quad (39)$$

with $F_1 = G$, $F_2 = Z$, and $F_3 = H$ and $i = 1, 2, 3$. The index j runs from 1 to N_{ch} , I are the integrals, and τ the remaining tree-level terms. Of course, an exact solution of the system satisfies $\vec{E} = \vec{0}$, and thus the aim is to find such a solution.

New values c'_{ij} for the coefficients are then obtained iteratively by [23]

$$\vec{c}' = \vec{c} - \lambda J^{-1} \vec{c}, \quad (40)$$

where \vec{c} is the vector of coefficients c_{ij} with the components $(\vec{c})_{(i-1)N_{ch}+j} = c_{ij}$. J is the Jacobian defined as

$$J_{ij} = \frac{\partial E_i}{\partial c_j}. \quad (41)$$

The stepwidth is determined by the backtracking parameter λ . It is chosen such as to minimize $|\vec{E}|$, where a simple quadratic interpolation has been used [23]: A first trial step is a full local Newton step ($\lambda = 1$). This is accepted, if it decreases the previous value $|\vec{E}| = r_0$. If this is the case, the algorithm has already moved so close to the correct solution that the faster local algorithm can be used (which provides quadratic instead of the linear convergence of the global version [23]).

If this not leads to a decrease, a trial step of size $\sigma_1 < 1$ is performed. If this again provides no reduction of $|\vec{E}|$, the quadratic interpolation is used: Given the step-size of the current trial step λ_2 and of the previous trial step λ_1 , leading to values r_2 and r_1 of $|\vec{E}|$, respectively, a new trial value of λ is determined by a quadratic interpolation using the first two terms of a Taylor expansion of $|\vec{E}|$ to construct [23]

$$p_1 = \frac{r_0(\lambda_2^2 - \lambda_1^2) - \lambda_1^2 r_2 + \lambda_2^2 r_1}{\lambda_1 \lambda_2^2 - \lambda_1^2 \lambda_2}$$

$$p_2 = \frac{(2\lambda_1 \lambda_2)(\lambda_2(r_1 - r_0) - \lambda_1(r_2 - r_0))}{\lambda_1 - \lambda_2}.$$

Thus if p_2 is greater than zero a descent direction is found, and the new value $\lambda = -p_1/p_2$ minimizes the Taylor series truncated at the quadratic order. However, the quadratic approximation may not be sufficient, leading to a step-width outside the interval $(0, \lambda_2]$ or may be too close to 0 or λ_2 to be reliable. Thus if the new λ lies outside the range $[\sigma_0 \lambda_2, \sigma_1 \lambda_2]$, with $\sigma_0 < \sigma_1$, the new value of λ is taken to be the corresponding border value, e. g. if the new value of λ would be larger than $\sigma_1 \lambda_2$ it is reduced to $\sigma_1 \lambda_2$. If p_2 is positive or zero, a quadratic approximation is not reliable, and the new trial step is selected as $\lambda = \sigma_1 \lambda_2$. With this new value of λ , a new trial step is performed. If still no decrease is found, this procedure is repeated until $|\vec{E}|$ is decreased, and the trial step is accepted and (40) is performed. This is repeated until convergence is achieved, which will be discussed below.

The method fails to converge if λ becomes less than a predetermined value α_G . In the present case α_G is essentially determined by empirical knowledge, but in general cases should be at least of the order of the machine precision. The values of σ_0 and σ_1 are tuning parameters for the algorithm, a specific choice is presented in subsection 3.5.

A significant problem⁸ is the determination of the coefficient A_G of the infrared asymptotic behavior (25) of the ghost dressing function G . Trying to incorporate it into the global Newton method failed. Hence this part is moved to an outside iteration: after each global Newton iteration, a new value of A_G is determined by requiring that the infrared solution D_G^I connects continuously to the intermediate function $f_G D_G^N$. In general this leads to a continuous but not to a continuously differentiable function until convergence has been achieved.

Therefore A_G has not yet its final value. Thus the condition (27) is not fulfilled. Hence to stabilize the system, A_Z is not determined by its functional relation to A_G , but left as a free parameter and determined in the same way as A_G . Even for A_H , where its final value is exactly known, it is more advantageous to let it as a free parameter to stabilize the numerical algorithm. The starting values for A_G , A_Z , and A_H are chosen such that the infrared solution and the intermediate momentum solution fit continuously after the initial c_{ij} have been set. After each global Newton run, the coefficients are refitted. Thus the Newton iteration is termed a micro-cycle while the fix-point iteration of the coefficients is termed macro-cycle.

This approach is feasible, as it turns out that the radius of convergence for the coefficients is significantly larger than for the Chebychev coefficients. A_G is strongly constrained by the vanishing of the inverse ghost dressing function in the infrared, thus determining A_Z and A_H by their exact solutions. In other cases possibly another global iteration for the coefficients would be necessary. Note that during the iteration the values of the A_F can change by several orders of magnitude, even if initial and final value are close by. Furthermore as (27) is not fulfilled with the initial values it makes no sense to run the global Newton method until it converges. Therefore after a number of steps N_N the Newton method is interrupted, if it did not yet converge, to make a new macro-cycle step and then start a new micro-cycle. After several macro-cycle steps the Newton method already converges, i.e. $|\vec{E}| < \delta_G$ for a fixed δ_G , in less than N_N steps. In the present case it was possible to choose N_N fixed. In more instable solutions an adaptive choice may be appropriate.

In addition, still slow convergence is encountered. To deal with it leads to the introduction of super-cycles: it turns out that convergence is extremely slow if ε is chosen already quite small from the beginning. In this case the presented initial values are far from the final ones, and only very small steps can be made [23]. Since the infrared regime and the finite momenta regime do separate in the system under investigation, it is possible to choose an ε larger than the final matching scale. The solutions then are not continuous differentiable at ε and

⁸ Special thanks to Claus Feuchter and Burghard Grüter for a very inspiring discussion on this topic.

the relation (27) is not fulfilled. Thus the independence of the coefficients A_F in the fitting procedure is important here as well. Using the previous solutions for a given ε as the input for a smaller one, it was possible to approach the correct solutions stepwise with sufficiently good convergence. Indeed, regularly only the first steps of the micro-cycle in the first one or two macro-cycle steps utilized the global properties of the method and afterwards local and thus quadratic convergence in $|\vec{E}|$ was achieved. This is repeated until (27) is satisfied to the required precision.

It is possible to reduce the number of necessary super-cycle steps drastically in two ways. One is an improvement of the fit functions D_F^U and f_F to include sub-leading corrections. This leads to the final form of equation (34) and the fits (35-37). The other is the introduction of damping in the determination of the A_F . To this end the new values A'_F providing a continuous fit between D_F^I and $f_F D_F^N$ are computed, but instead setting the value of A_F'' in the next step to A'_F , only a variable admixture of A'_F to the original A_F is chosen as

$$A_F'' = \frac{dA_F + A'_F}{d + 1}, \quad (42)$$

where $d \geq 0$ is the damping parameter.

To test whether the algorithm has succeeded, two different criterions for the micro- and macro-cycle are used. For a micro-cycle the absolute value of $|\vec{E}|$ is used. The typical scale of terms is set by the tree-level term of order 1. Compared to this scale a mean deviation of the order 10^{-8} is achieved with the described numerical parameters. The largest deviation are usually found in the far infrared of equation (11), where diverging terms have to cancel and thus very high accuracy is necessary.

If the available precision is not sufficient, the necessity for these cancellations is also a limiting factor for the algorithm. An example of this problem is encountered when $\zeta \approx 3$ in case of the varying solution branch described in subsection 3.1. In this case, the divergencies of the two competing terms are softened, and thus very small values of ε are necessary before only the infrared leading terms are relevant and thus the asymptotic infrared solution D_F^I is sufficient. If ζ is sufficiently close to 3, the required values of ε are so small that the cancellations cannot be resolved with the available precision and the algorithm fails to converge.

For the macro-cycle the largest rate of change of the A_F is used as a measure of convergence. Typical when the rate of change is below a fixed value δ_I of the order of a per mill the macro-cycle is completed. For the super-cycle the ratio $A_G^2 A_Z / J(\zeta, e_G)$ according to (27) is used⁹. Note that due to numerical

⁹ The value of A_H is always so close to the final value that this is not a relevant

errors it is even with a machine precision of 10^{-16} only possible to fulfill (27) to the order of 10^{-5} .

3.4 Notes on implementation and optimization

While the implementation of the macro- and super-cycles is straightforward, there are some subtleties concerning the implementation of the micro-cycle. Once the values of the A_F are fixed in the macro-cycle, calculating the current value of the right hand sides of the DSEs is straightforward numerically. However, as the evaluation of the exponentials in the fits of the F is numerically costly, it is much more efficient to calculate all equations for a given p_j simultaneously, as here the same set of Gauss-Legendre points can be used.

This issue is much more important when performing the Newton step. To determine the descent direction for the coefficients c_{ij} , it is necessary to calculate the Jacobian. As this Jacobian contains the derivatives of the equations (39) with respect to the coefficients¹⁰ c_{ij} , each element contains essentially a two-dimensional integration. Calculating therefore each element one-by-one is extremely inefficient. It is therefore advantageous to evaluate all elements with fixed p_j simultaneously for all derivatives, corresponding to a complete column in parallel. This parallelism is implemented by performing one addition of the Gauss-Legendre integration for each of the equations simultaneously by summing in an appropriate vector. Therefore it is also not possible to use standard Gauss-Legendre integrators from libraries, as they usually do not allow in a two dimensional array efficient parallel summation for a vector of integrals with appropriate treatment of input functions like the dressing functions.

The performance can be enhanced further by close inspection of the system under consideration. In the case of equations (9-11) it can be exploited that inside the integrals one of the dressing function does not depend on the integration angle. Excluding it from the angular integration also improves the cancellation of divergencies, thus reducing the required number of angular integration points. The same applies to factors of T_j in the calculation of the Jacobian matrix.

Compared to the time necessary to calculate the Jacobian, all other elements are completely subleading. Therefore it is no advantage to use an approximate inversion routine to speed up the calculation of the inverse Jacobian for the Newton step. The gain in speed does not outweigh the drawback in precision. It is furthermore useful to store the inverted Jacobian and not to recalculate

figure of merit.

¹⁰ Note that the derivative of $\exp(c_{ij}T_j)$ w.r.t. the c_{ij} is $T_j \exp(c_{ij}T_j)$. Hence no costly numerical derivatives of the dressing functions are necessary.

C_A	g_3^2	δ_{3g}	ζ	m_h	m_r	e_G	e_Z
3	1	1/4	1	$0.8808g_3^2$	$0.9930g_3^2$	0.39760	-1.2952

Table 2

The physical parameters in the example run.

δ	ε	Λ	Ω	N_{ch}	N_a	N_δ	N_ε	α_G
$10^{-6}g_3^2$	$0.0201193g_3^2$	$99407.2g_3^2$	$10^7g_3^2$	39	80	60	100	10^{-5}
σ_1	σ_0	δ_G	N_N	d	δ_I	N_p	N_Λ	
0.5	0.1	10^{-8}	5	2	10^{-5}	100	60	

Table 3

The numerical parameters in the example run.

Initial A_G	1.06894	Final A_G	0.838007
Initial A_Z	0.99109	Final A_Z	13.4111
Initial A_H	1.01411	Final A_H	1.01404
Initial ratio $A_G^2 A_Z / J(\zeta, e_G)$	0.12035	Final ratio $A_G^2 A_Z / J(\zeta, e_G)$	1.0019
Initial ratio A_h^2 / m_r^2	1	Final ratio A_h^2 / m_r^2	0.99993
Initial $ \vec{E} $	3.6×10^5	Final $ \vec{E} $	2.5×10^{-9}
Final rate of change of A_G	7.9×10^{-6}	Number of micro-cycles	25

Table 4

The initial and final values for the infrared coefficients together with some run statistics. The run time was about 20 minutes on a 2.8 GHz Intel Xeon processor.

it during the backtracking, as it does not change. Using all these optimization gives a factor of roughly 30-60 in speed.

3.5 Example calculation

Here the results for an example calculation will be presented. The physical parameters are listed in table 2. The numerical parameters can be found in table 3 and the initial values along with the final values and run parameters in table 4. The final values for the coefficients c_{ij} are not displayed. Initially they have been set to 0. Using these parameters results have been obtained in a single super-cycle step.

The results are presented in figures 1-3 for the ghost, gluon, and Higgs dressing functions, respectively. Along the various final fitting functions in (34) are shown. Together with the results in table 4 this demonstrates the abilities of the method in a most direct way. Note especially that the mismatch measured by $|\vec{E}|$ is decreased by 14 orders of magnitude. Up to 18 orders have also been

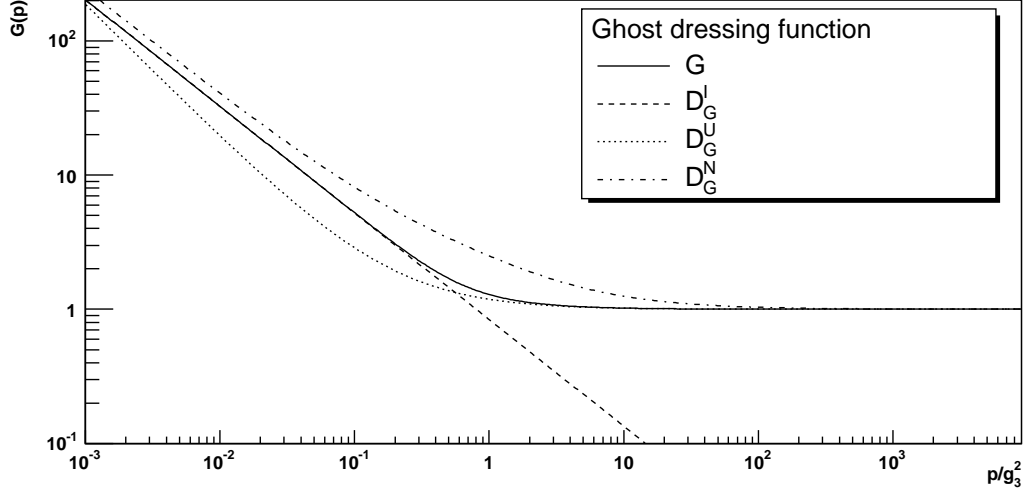


Fig. 1. The ghost dressing function compared to the infrared, intermediate, and ultraviolet fitting functions.

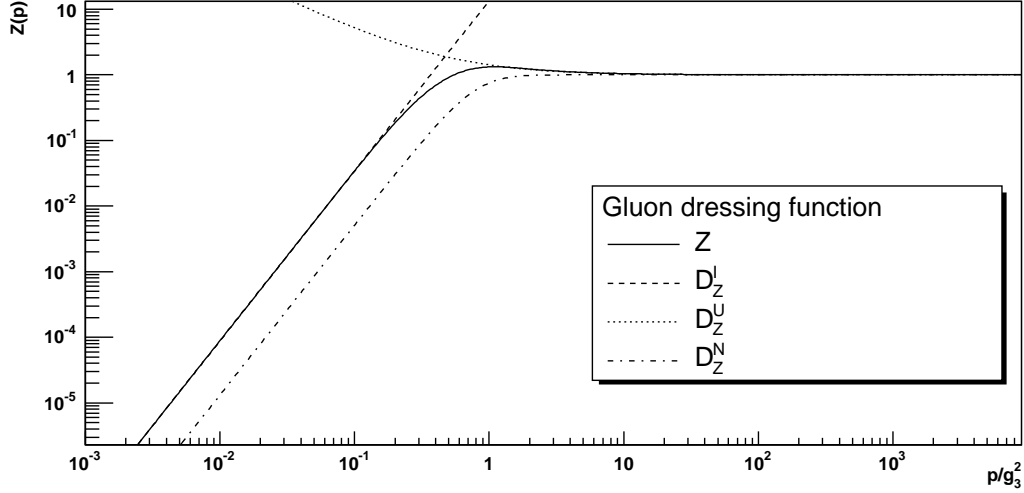


Fig. 2. The gluon dressing function compared to the infrared, intermediate, and ultraviolet fitting functions.

achieved. Further examples can be found in refs. [7,8,9].

4 4-dimensional Yang-Mills theory

In case of the renormalized system (15-17), the main qualitative change is the appearance of the renormalization constants, defined in equations (18-24). Especially the infrared properties of the $p_0 = 0$ modes do not change [7,9]. In the ultraviolet the coefficients in (28) change, but this effect can be ignored. In fact the subleading term is completely dropped and only the leading term is (and must be) retained. The $p_0 \neq 0$ modes become constant both in the

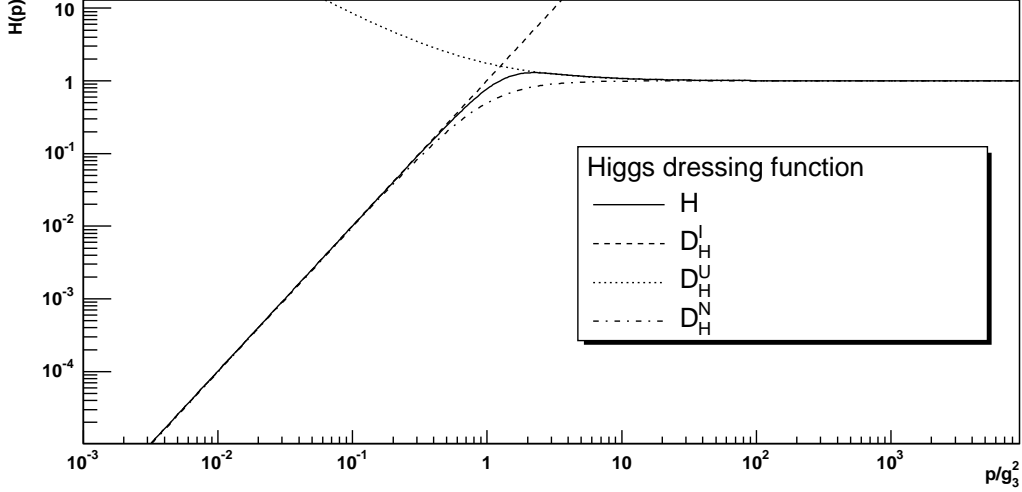


Fig. 3. The Higgs dressing function compared to the infrared, intermediate, and ultraviolet fitting functions.

infrared and the ultraviolet.

If the renormalization constants would only appear explicitly as in equations (15-17), then the most direct implementation would be to treat them on equal footing with the remaining integrals. Although this would add $3N_{ch}$ integrals when evaluating the Jacobian, this would be a subleading effect. However, the constants cannot be kept the same during a complete Newton iteration. Although the system is finite, the effect of renormalization is still large and the would-be divergencies would lead to solutions which are incorrect, thus slowing the convergence significantly if not leading to divergence.

In addition, this is not the only effect. Due to the truncations made [7,9], it is necessary in nearly all integrals to replace the factor $F(q_0, \vec{q})F(p_0 \pm q_0, \vec{p} \pm \vec{q})$ by¹¹

$$\left(F(q_0, \vec{q}) - \frac{1}{Z_3(q_0)}\right) \left(F(p_0 \pm q_0, \vec{p} \pm \vec{q}) - \frac{1}{Z_3(p_0 \pm q_0)}\right). \quad (43)$$

Therefore the renormalization constants appear in a non-trivial combination, which are especially cumbersome when derivatives with respect to the c_{ij} are performed. Although this problem could also be dealt with by determining the renormalization constants and their derivatives once for each N_{ch} set of equations, a more direct approach is possible. For a single Newton step, it is viable to keep the renormalization constants fixed. Then afterwards new renormalization constants are determined and the next Newton step is performed. Therefore each Newton iteration is split into sub-iterations, each of one step length, which is repeated in a micro-cycle for N_N steps or until convergence has been achieved. Due to the global convergence of the Newton method this

¹¹ Z_3 is again the generic wave-function renormalization constant of the dressing function F .

is permissible and quite efficient, as the renormalization constants not change drastically within one Newton step. This strategy may not be possible in cases where these constants do change appreciably. In the present case, this is the most efficient solution. This is important, as now $3NN_{ch}$ equations have to be solved. With this method, a system of $N = 20$ and $N_{ch} = 60$ (yielding a Jacobian with about 10^7 entries) converges without further prior knowledge within a few days on a 2.8 GHz Intel Xeon.

5 Conclusions

In this work a globally convergent method was presented to solve coupled sets of nonlinear integral equations. The example investigated are DSEs for Yang-Mills theories. Equipped with qualitative knowledge of the infrared and ultraviolet properties only, it was possible to solve the system without further prior knowledge with an acceptable efficiency. Most crucial to this efficiency is the careful optimization of the calculation of the Jacobian inside the global Newton method, which is at the heart of the algorithm.

The approach showed global convergence, thus extending earlier local algorithms, and therefore provides the abilities to solve such sets of equations without referring to other methods to provide good initial guesses. It will therefore be useful in the further investigations of DSEs and similar mathematical problems.

However, the method relies crucially on knowledge of the asymptotic behavior. Attempts to at least remove the need for the infrared behavior have failed so far, although many different methods have been tried, ranging from expansion in suitable characteristic functions up to genetic algorithms. In many physical cases these asymptotics are known, but especially in gauge theories this is usually not yet the case in general gauges, see e.g. [24]. Therefore it remains desirable to construct such a numerical continuum method.

Acknowledgments

The author is grateful to R. Alkofer, C. Feuchter, C. S. Fischer, B. Grüter, and S. Roch for many helpful discussions and is indebted to R. Alkofer, C. S. Fischer and D. Nickel for a careful reading of the manuscript and helpful comments. This work is supported by the BMBF under grant number 06DA917 and 06DA116, and by the Helmholtz association (Virtual Theory Institute VH-VI-041).

A Integral kernels and tadpoles of the 3-dimensional System

The integral kernels in (9-11) are obtained using standard methods [1,7,8]. They depend only on the magnitude k and q and the relative angle θ between their two momentum arguments. The kernel in the ghost equation (9) is given by

$$A_T(k, q) = -\frac{q^2 \sin^3(\theta)}{(k^2 + q^2 - 2kq \cos \theta)^2}.$$

The contributions in the Higgs equation (10) are

$$N_1(k, q) = -\frac{2q^2 \sin^3(\theta)}{(k^2 + q^2 + 2kq \cos \theta)^2} \quad (\text{A.1})$$

$$N_2(k, q) = -\frac{2 \sin^3(\theta)}{k^2 + q^2 + 2kq \cos \theta}. \quad (\text{A.2})$$

The kernels in the gluon equation (11) are finally

$$R(k, q) = -\frac{((\zeta - 1)kq \cos(\theta) - q^2 + \zeta q^2 \cos^2(\theta)) \sin \theta}{2k^2(k^2 + q^2 + 2kq \cos \theta)}$$

$$M_L(k, q) = \frac{((\zeta - 1)(k^2 + 4kq \cos \theta) - 4q^2 + 4q^2 \zeta \cos^2(\theta)) \sin \theta}{4k^2(k^2 + q^2 + 2kq \cos \theta)} \quad (\text{A.3})$$

$$M_T(k, q) = \frac{\sin \theta}{4k^2(k^2 + q^2 + 2kq \cos \theta)} \left((k^2 + 2q^2)((\zeta - 9)k^2 - 4q^2) \right. \\ \left. + 8(\zeta - 3)(k^2 + q^2)kq \cos \theta + (8\zeta q^4 + (\zeta + 7)k^4) \right. \\ \left. + 4(5\zeta - 1)k^2 q^2 \cos^2(\theta) + 4(4\zeta q^2 + (\zeta + 3)k^2) \cos^3(\theta) \right. \\ \left. + 4\zeta k^2 q^2 \cos^4(\theta) \right). \quad (\text{A.4})$$

The modified gluon vertex is introduced by multiplying M_T with

$$(A(q, G, Z)A(q + k, G, Z)A(k, G, Z))^{\delta_{3g}} \quad (\text{A.5})$$

where $A(q, G, Z)$ is given by

$$A(q, G, Z) = \frac{1}{Z(q)G(q)^{2+\frac{1}{2\epsilon_G}}}. \quad (\text{A.6})$$

The tadpoles used read:

$$\begin{aligned}
T^{GG} = & -\frac{g_3^2 C_A}{(2\pi)^2} \int dq d\theta \left(R_D(p, q) (G(q)G(p+q) - A_G^2 q^{-2e_G} (p+q)^{-2e_G}) \right. \\
& + R_3(p, q) (G(q)G(p+q) - A_G^2 q^{-2e_G} (p+q)^{-2e_G} - 1) \\
& \left. + M_{TD}(p, q) Z(q) Z(p+q) \right). \tag{A.7}
\end{aligned}$$

Here the kernel R has been split into a convergent, ζ -independent part R_0 , its divergent part R_D , and a remaining part R_3 as

$$R = R_0 + (\zeta - 3)R_3 + R_D. \tag{A.8}$$

The divergent parts are in general isolated by

$$R_D(p, q) = \lim_{q \rightarrow \infty} R(p, q). \tag{A.9}$$

M_{TD} contains the divergent part of M_T , including the modifications due to the dressed 3-gluon-vertex (A.5). The other tadpole in the gluon equation is given by

$$T^{GH} = -\frac{g^2 C_A}{(2\pi)^2} \int dq d\theta \left(M_{LD}(p, q) H(q) H(p+q) \right). \tag{A.10}$$

Again, M_{LD} contains the divergent part of M_L . In the Higgs equation, the tadpoles are set to

$$T^{HG} + T^{HH} = \frac{g_3^2 C_A}{p^2} \frac{m_h}{4\pi}. \tag{A.11}$$

A detailed account for the construction of the tadpoles is given in ref. [7].

References

- [1] R. Alkofer and L. von Smekal, Phys. Rept. **353** (2001) 281 [arXiv:hep-ph/0007355].
- [2] A. D. Polyanin, A. V. Manzhirov, “Handbook Of Integral Equations”, CRC Press, Boca Raton, 1998 and german translation, Spektrum-Verlag, Heidelberg, 1999 and references therein.
- [3] C. S. Fischer, R. Alkofer and H. Reinhardt, Phys. Rev. D **65** (2002) 094008 [arXiv:hep-ph/0202195].
- [4] B. Grüter, R. Alkofer, A. Maas and J. Wambach, Eur. Phys. J. C **42** (2005) 109 [arXiv:hep-ph/0408282].
- [5] C. S. Fischer, B. Gruter and R. Alkofer, arXiv:hep-ph/0506053.
- [6] C. S. Fischer, PhD thesis, University of Tübingen, November 2002, arXiv:hep-ph/0304233.

- [7] A. Maas, PhD thesis, Darmstadt University of Technology, October 2004, arXiv:hep-ph/0501150.
- [8] A. Maas, J. Wambach, B. Grüter and R. Alkofer, Eur. Phys. J. C **37** (2004) 335 [arXiv:hep-ph/0408074].
- [9] A. Maas, J. Wambach and R. Alkofer, Eur. Phys. J. C **42** (2005) 93 [arXiv:hep-ph/0504019].
- [10] F. J. Dyson, Phys. Rev. **75** (1949) 1736, J. S. Schwinger, Proc. Nat. Acad. Sci. **37** (1951) 452, Proc. Nat. Acad. Sci. **37** (1951) 455.
- [11] R. J. Rivers, “Path Integral Methods In Quantum Field Theory,” Cambridge, UK: Univ. Pr. (1987) 339 p. (Cambridge monographs on mathematical physics).
- [12] M. Bohm, A. Denner and H. Joos, “Gauge Theories Of The Strong And Electroweak Interaction,” Stuttgart, Germany: Teubner (2001) 784 p.
- [13] K. Kajantie, M. Laine, K. Rummukainen and M. E. Shaposhnikov, Nucl. Phys. B **458** (1996) 90.
- [14] A. Cucchieri, F. Karsch and P. Petreczky, Phys. Rev. D **64** (2001) 036001 [arXiv:hep-lat/0103009].
- [15] V. N. Gribov, Nucl. Phys. B **139** (1978) 1. D. Zwanziger, Phys. Rev. D **69** (2004) 016002 [arXiv:hep-ph/0303028].
- [16] J. I. Kapusta, “Finite Temperature Field Theory”, Cambridge University Press, Cambridge (1989).
- [17] A. Hauck, L. von Smekal and R. Alkofer, Comput. Phys. Commun. **112** (1998) 149 [arXiv:hep-ph/9604430]. A. Hauck, L. von Smekal and R. Alkofer, Comput. Phys. Commun. **112** (1998) 166 [arXiv:hep-ph/9804376].
- [18] D. Atkinson and J. C. R. Bloch, Phys. Rev. D **58** (1998) 094036 [arXiv:hep-ph/9712459].
- [19] C. S. Fischer and R. Alkofer, Phys. Lett. B **536** (2002) 177 [arXiv:hep-ph/0202202].
- [20] C. Lerche and L. von Smekal, Phys. Rev. D **65** (2002) 125006 [arXiv:hep-ph/0202194]; D. Zwanziger, Phys. Rev. D **65** (2002) 094039 [arXiv:hep-th/0109224].
- [21] L. von Smekal, R. Alkofer and A. Hauck, Phys. Rev. Lett. **79** (1997) 3591 [arXiv:hep-ph/9705242]; L. von Smekal, A. Hauck and R. Alkofer, Annals Phys. **267** (1998) 1 [Erratum-ibid. **269** (1998) 182] [arXiv:hep-ph/9707327].
- [22] J. C. R. Bloch, PhD thesis, Durham University, November 1995, arXiv:hep-ph/0208074.
- [23] C. Kelley, “Iterative methods for linear and non-linear equations”, Siam, Philadelphia: Siam (1995).
- [24] R. Alkofer, C. S. Fischer, H. Reinhardt and L. von Smekal, Phys. Rev. D **68** (2003) 045003 [arXiv:hep-th/0304134].